Characterization of Axonal Spikes in Cultured Neuronal Networks Using Microelectrode Arrays and Microchannel Devices

Nari Hong, Sunghoon Joo, and Yoonkey Nam*, *Member, IEEE*

Abstract*—*Objective: **Axonal propagation has a pivotal role in information processing in the brain. However, there has been little experimental study due to the difficulty of isolation of axons and recording their signals. Here, we developed dual chamber neuronal network interconnected with axons by integrating microchannel devices with microelectrode arrays (MEAs) to investigate axonal signals in developmental stage.** ***Methods:*** **The device was composed of two chambers and microchannels between them, and hippocampal neurons were cultured in both chambers. Neuronal activity was recorded for four weeks.** ***Results:*** **Large axonal signal was detected in microchannels, which were 137.0 $\pm$ 8.5 μV at 14 days *in vitro* (DIV). It was significantly larger than those in chambers with a similar range of signal-to-noise ratio. Detection efficiency of axonal spikes was analyzed by calculating the number of active electrodes over time. We found that active electrodes were detected earlier and their number increased faster in microchannels than those in chambers. Finally, we estimated the axonal conduction velocity and 73% of axons had the velocity in range of 0.2–0.5 m/s at 14 DIV. By estimating the velocity over the cultivation period, we observed that axonal conduction velocity increased linearly over time.** ***Conclusion:*** **Using MEAs and microchannel devices, we successfully detected large axonal signals and analyzed their detection efficiency and conduction velocity. We first showed the gradual increase in conduction velocity depending on cultivation days.** ***Significance:*** **The developed microchannel device integrated MEA may be applicable for the studies of axonal conduction in cultured neuronal networks.**

***Index Terms*—Axonal spikes, conduction velocity, microchannel device, microelectrode array (MEA), neural recording.**

I. Introduction

NEURAL network is composed of functionally connected modules. Between modular networks, axons propagate and modulate action potentials generated in one module to other modules like transmission cables [1]–[3]. To investigate mechanisms of information processing in neural networks, microelectrode arrays (MEAs) are widely used to record extracellular signals from *in vitro* neuronal networks and analyze their electrophysiological properties since they enable long-term noninvasive and spatiotemporal recording. However, it has been challenging to access axons to measure their action potentials because the signals from axons, which have small diameters, are much smaller than those of somata. In order to deal with this challenge in terms of the spatial resolution of MEAs which is limited by the areal density of electrodes, high-density MEA was newly developed for detecting and tracking axonal spikes [4].

Recently, a new method to isolate axons from neural network was suggested using a microchannel device fabricated with polydimethylsiloxane (PDMS) [5], [6]. The device consisted of two large chambers and interconnecting microchannels which had the cross-sectional profile of $3\,\mu\text{m} \times 10\,\mu\text{m}$ for selective axonal outgrowth. Integration of this device with a planar-type MEA by aligning microchannels onto the electrodes of an MEA provided an innovative platform to access axonal signals in the network. Extraordinarily large action potentials from isolated bundles of axon were recorded due to the high end-to-end resistance, and axonal conduction velocity was estimated from the recorded signals [7], [8]. Using the dual chamber devices, velocities at proximal and distal part of axons were detected separately, and the velocity decrease with increasing culture days was observed only at the distal part [9]. With the same device, it was demonstrated that the axonal conduction velocity decreased during one network burst [10]. The microchannel device integrated on an MEA was also used to analyze the direction of propagation between networks. By sequential cell plating, unidirectional connectivity was established and the signal propagation in intended direction was successfully recorded from 84% of spikes [11]. Self-wiring of trisynaptic pathway, especially from DG to CA3, was demonstrated by plating cells from each subregion into separated chambers [12]. Although the platform is actively applied to MEAs for various experiments, axonal signals in the network has not been fully explored. In previous researches, most of them did not consider the change of axonal signals over time even though this platform gives us an opportunity to evaluate the conduction through the axons during the developmental periods of several weeks.

Manuscript received February 15, 2016; revised April 4, 2016; accepted May 4, 2016. Date of publication May 12, 2016; date of current version January 18, 2017. This work was supported by National Research Foundation under Grant (NRF-2012R1A2A1A01007327, NRF-2015R1A2A1A09003605) funded by Korean government. *Asterisk indicates corresponding author.*

N. Hong and S. Joo are with the Department of Bio and Brain Engineering, Korea Advanced Institute of Science and Technology.

*Y. Nam is with the Department of Bio and Brain Engineering, Korea Advanced Institute of Science and Technology, Daejeon 34141, South Korea (e-mail: ynam@kaist.ac.kr).

Digital Object Identifier 10.1109/TBME.2016.2567424

Here, we investigated axonal recordings from two-compartment neuronal network in developmental stage using the microchannel integrated MEA platform. From recorded axonal signals, we analyzed their characteristics and conduction velocity through the axons to address the following questions: 1) Is there any difference between axonal signals from microchannels and those from open chambers in terms of their signal-to-noise ratio (SNR) as well as amplitude? 2) Does the efficiency of spike detection alter during the network development? 3) How does the axonal conduction velocity change as the network get matured? To investigate these questions, we designed an attachable microchannel device with a planar-type MEA that is composed of two millimeter-sized chambers connected by 50 microchannels. In both chambers of the device, hippocampal neurons were cultured and their activitities were sampled every one or two days for four weeks. With two-compartment neuronal network interconnected with axons on an MEA, we measured neuronal signals from microchannels and chambers to compare their properties such as amplitude, background noise, and SNR. Then, we analyzed detection efficiency of axonal signals by calculating the number of active electrodes and their trend over time. From axonal spikes, we estimated the conduction velocity between compartmental networks and their changes during the network development. We found that larger axonal spikes can be detected in microchannels with reasonable SNR value and high detection efficiency. The conduction velocity of signal propagation via axons increased as the cultivation time increases.

II. Methods and Materials

A. Microchannel Device Fabrication and Integration on an MEA

An MEA was fabricated through foundry service provided by National Nanofab Center (Daejeon, South Korea). Conductor lines were composed of 20-nm-thick titanium film and 200-nm-thick gold film, and they were insulated by 500 nm-thick PECVD (plasma-enhanced chemical vapor deposition) silicon nitride film. The size of electrodes was 30 μm or 50 μm in diameter with 200 μm spacing in 8 by 8 grid layout. The MEA had 59 microelectrodes and one large reference electrode (area: 1.4×2.7 mm^2).

A two-chamber microchannel device was fabricated through soft-lithography. A SU-8 mold was made by two-mask photolithography step. Microchannel parts were made in the first step. SU8-2002 (MicroChem, MA, USA) was spun on a four-inch silicon wafer at 500 rpm for 10 s and 1000 rpm for 30 s to obtain the thickness of 3 μm. Then, the wafer was soft-baked and exposed to UV light with the first mask for 8 s at 15 mW/cm^2. After hard-baking and development, 3 μm thin structures were formed. Next, two culture chambers were made in the second step using a thick photoresist. SU8-2050 (MicroChem, MA, USA) was spun for the 120 μm thickness of layer. The second mask was aligned and the wafer was exposed to UV light for 24 s at 15 mW/cm^2. Once the SU-8 was completed, the master mold was coated with silane (Trichloro(1H, 1H, 2H, 2H-perfluorooctyl)silane, Aldrich, MO, USA) in a desiccator for 45 min to facilitate PDMS mold release. Then, the mixture of PDMS prepolymer and curing agent (Sylgard 184, Dow Corning, MI, USA) was poured onto the mold and degassed in a desiccator. Then, after it was cured at 60 °C in an oven for at least 2 h, the cured PDMS was peeled off and cut into individual devices. For each device, two rectangular holes were punched and the whole device was treated with air plasma (Cute, Femto Science, Hwaseong, South Korea) for 5 min to make their surface hydrophilic. The device was attached on an MEA with an assist of visual alignment under stereo microscope (SZ61, Olympus, Japan) in such a way that two electrodes columns were placed in microchannels.

Before aligning the device, the surface of MEA was coated with polydopamine (2 mg/mL in 10 mM Tris buffer, pH 8.5, Sigma-Aldrich, MO, USA) for 1 h. Then, the surface was rinsed with DI and treated with air plasma for 1 min. Lastly it was coated with poly-D-lysine (0.1 mg/mL in 10 mM Tris buffer, pH 8.5, Sigma-Aldrich, MO, USA) for 1 h for neural cell adhesion.

B. Cell Culture

Hippocampi were dissected from E18 Sprague-Dawley rat (Koatech, Pyeongtaek, South Korea) and they were rinsed with Hank's buffer salt solution (HBSS, Welgene, Daegu, South Korea), followed by dissociation using pipettes. They were centrifuged for 2 min at 1000 rpm and the supernatant was replaced with plating medium consisting of Neurobasal medium (Gibco, CA, USA), B27 supplement (Gibco, CA, USA), 2 mM of GlutaMAX (Gibco, CA, USA), 12.5 μM of L-glutamate (Sigma-Aldrich, MO, USA), and 1% penicillin-streptomycin (Gibco, CA, USA). Using a cell strainer (BD Falcon, NJ, USA), the cell suspension was filtered and then cells were plated in two chambers at the density of 1000–1500 cells/mm^2. At 3 days *in vitro* (DIV), the plating medium was changed to maintenance medium which did not contain L-glutamate. Half of the medium was replaced with fresh medium every 5 days. The cell culture was maintained in a humidified incubator (5% CO_2 and 37°C). Inverted microscopy (IX71, Olympus, Japan) with digital camera (DP71, Olympus, Japan) using a 20X objective lens was used for phase-contrast.

C. Neural Signal Recording

Neural signals were recorded from the cultured networks on MEAs at 9–28 DIV. To record from the networks, MEAs were connected with an amplifier (Custom-built, Gain: 1000, bandwidth: 150–4500 Hz) and signals were digitized using MC Card (sampling frequency: 25 kHz, Multichannel Systems, Germany). A gold reference electrode integrated on the MEA was connected with the amplifier ground. During the 10-min recording session, cultures were maintained under 37°C and 5% CO_2 condition by putting the MEA on a temperature controller and covering them with a CO_2 gas cap.

D. Data Analysis

From the recorded data for 10 min, spikes were detected by setting the threshold level (-8 x standard deviation) using

MC_Rack software (Multichannel Systems, Germany). And they were clustered in a 3D feature space (PC1, PC2, and PC3) by valley-seeking algorithm using OfflineSorter (Plexon Inc., Dallas, TX, USA).

For the quantification of axonal velocity, the cross-correlation based analysis was performed using MATLAB (MathWorks Inc., MA, USA) and Neuroexplorer (Nex Technologies, AL, USA). Cross correlograms of sorted units in a same microchannel were obtained with the analysis time window and bin size 1 ms and 40 μs, respectively.

All statistical data was presented in mean and standard error of mean (SEM) and statistical analyses were performed using GraphPad Prism (GraphPad Software Inc., CA, USA) with confidence intervals of 99%.

III. Results

A. Integration of a Microchannel Device on an MEA

Fig. 1(b) shows a drawing of a PDMS microchannel device on an MEA. The PDMS device was composed of two large chambers (3 mm $\times$ 3 mm, depth: 2 mm) and 50 microchannels (width: 10 μm, height: 3 μm, length: 400 μm). According to the original report on the device design by Jeon *et al*., the channel height had to be sufficiently small so that cell bodies cannot migrate into the microchannel [5], [6], whereas the channel length had to be long enough so that dendrites will not reach the other chamber. Considering these requirements, we used the height of 3 μm and the channel length of 400 μm to achieve axonal isolation in microchannels from two-compartmental networks.

Fig. 1(c) shows a phase-contrast image of a PDMS device aligned with an MEA. Among 50 microchannels which were equally spaced by 30 μm, 8 center-channels contained a pair of microelectrodes to measure axonal spikes. The rest of the electrodes were placed in left and right chambers to measure spikes from each compartment. There was a roof area (height: 120 μm) at the entrance of microchannels due to the hole punching process.

B. Long-Term Cultivation of Neurons on Integrated Platform

E18 rat hippocampal neurons were seeded in two chambers and cultivated for four weeks. During the 4-week cultivation, neurons were well maintained in two chambers and axons followed the microchannels to connect the networks in two chambers. Fig. 2(a) shows a representative example of neuronal growth in microchannels and chambers at 28 DIV. In microchannels, only neurites were observed and neurons seeded in chambers formed dense networks as shown in Fig. 2(a). Spontaneous activity in microchannels and chambers can be detected until four weeks after cultivation. Axons in microchannels were intact for four weeks. Fig. 2(b) shows phase contrast images of axonal outgrowth, which was marked in red dash lines, taken at different time points between one week and four weeks. At 9 DIV, a thin and dim line considered as axons was observed. At 14 DIV and 21 DIV, the line became thicker and clearer, and it retained its shape until 28 DIV.

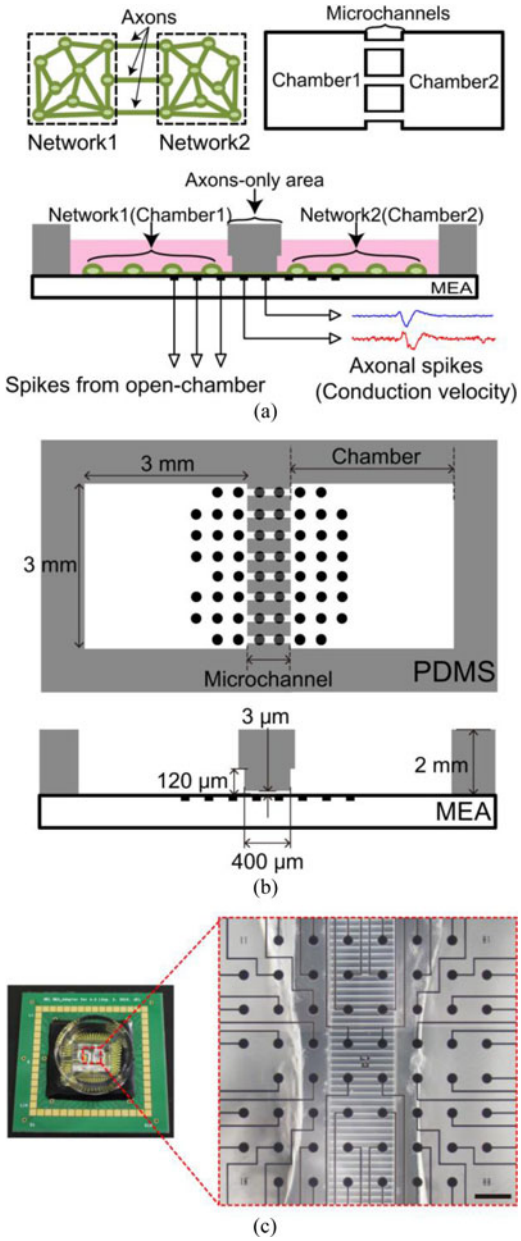

Fig. 1. (a) Overview of experimental design. (b) Schematic of top view and cross-sectional view. (c) Microscopic image of integrated platform. Scale bar: 200 μm.

C. Evaluation of SNR From Microchannels

Fig. 3(a) shows the raw traces of electrical signals at 14 DIV recorded from microelectrodes located at a microchannel and a chamber, respectively. To evaluate the quality of signals from microchannels, we compared neural signals from microchannels and chambers in terms of spike amplitudes and background noise levels at 14 DIV.

Spike amplitudes in microchannels were $137.0 \pm 8.5\,\mu$V (mean $\pm$ SEM, $N = 189$ units from 80 electrodes), whereas those from chambers were $72.2 \pm 3.0\,\mu$V (mean $\pm$ SEM, $N = 278$ units from 111 electrodes). Spikes from microchannels were significantly larger than those from chambers [see Fig. 3(b), $^{***}p < 0.001$], which was consistent with the previous report

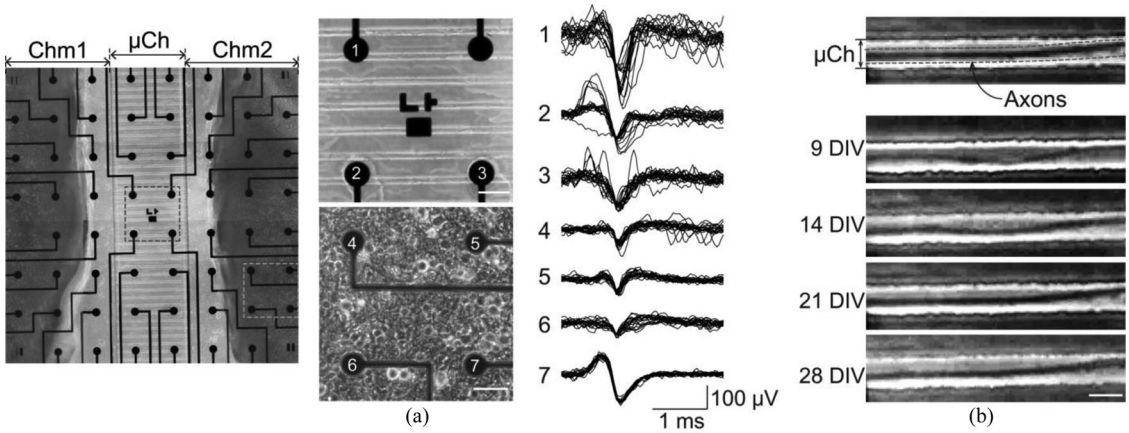

Fig. 2. Long-term cultivation of neurons in integrated platform. (a) Phase-contrast images of neuronal network and spikes from each electrode in microchannels and chambers at 28 DIV. Scale bar: 50 μm. (b) Phase-contrast images of axonal outgrowth marked in red dash lines at 9, 14, 21, 28 DIV. Scale bar: 10 μm.

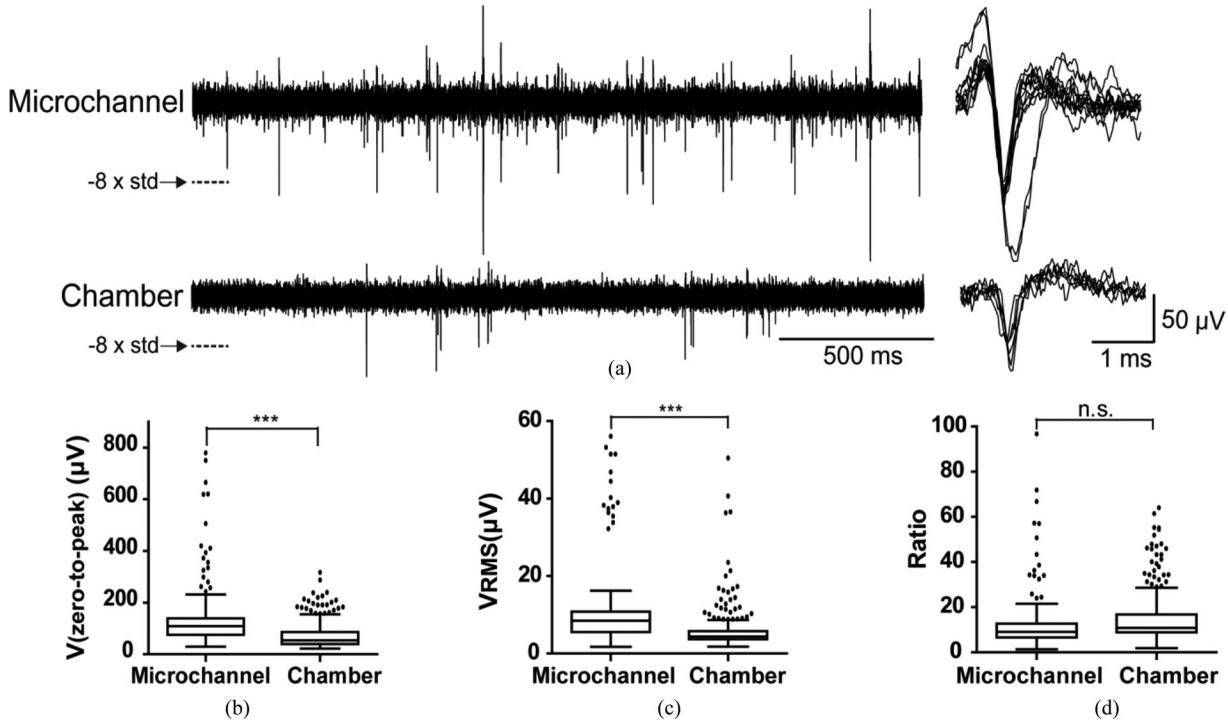

Fig. 3. Characterization of MEA signals from microchannels and chambers. (a) Raw trace and detected spikes of recorded signals. Thresholds of spike detection are denoted by arrows. (b) Statistical analysis of spike amplitude (zero-to-peak), (c) RMS of noise, and (d) SNR. Tukey box plots for $N = 66$ units from 80 electrodes (Microchannel) and 278 units from 111 electrodes (Chamber). The box bounds the first and third quartiles, and Tukey-style whiskers extend to 1.5 times interquartile range. Two tailed unpaired *t*-test; $^{***}p < 0.001$.

[7]. In case of the root-mean-square (RMS) value background noise level, microelectrodes in microchannels had significantly higher noise level than those in chambers [see Fig. 3(c)]. RMS values of background noise were $11.0 \pm 0.8\,\mu$V (mean $\pm$ SEM, $N = 80$ electrodes) in microchannels and $5.3 \pm 0.2\,\mu$V (mean $\pm$ SEM, $N = 111$ electrodes) in chambers. In order to find the account for the increased noise level, we measured the series resistance from ground to the electrode. For the microchannel electrodes, the series resistance was 1.9 ± 0.1 MΩ (mean $\pm$ SEM, $N = 15$ electrodes, $f = 1$ kHz), whereas that of chamber electrodes was 102.5 ± 3.4 kΩ (mean $\pm$ SEM, $N = 38$ electrodes, $f = 1$ kHz). Theoretical RMS values of noise level calculated from these resistances were $11.9\,\mu$V in microchannels and $2.8\,\mu$V in chambers. The measured RMS noise of microchannels was very similar to the estimated value, whereas the noise of chambers was measured slightly higher than the theoretical value. In Fig. 3(d), the SNR values were calculated as the spike amplitude divided by noise RMS value, which were estimated to be 13.2 ± 1.1 (mean $\pm$ SEM, $N = 189$ units from 80 electrodes) in microchannels and 15.4 ± 0.7 (mean $\pm$ SEM, $N = 278$ units from 111 electrodes) in chambers. There was no significant difference in SNR values from the two groups of microelectrodes, but the absolute level of SNR values were adequate for the detection of axonal spikes without an averaging

method that is used in open-chamber conditions [4]. It should be noted that these two SNR values can be derived from different types of signals because the detected spikes in microchannels most likely resulted from axons, whereas those in chambers were more likely from axon initial segments. Thus, the SNR value in microchannels cannot easily be compared with that in chambers, and the value of microchannels will be much larger in comparison with a SNR value for only axonal signals in chambers.

D. Analysis of Spike Detection Efficiency in Developing Neuronal Networks

In order to find out how detection efficiency of axonal spiking activity changes during the network development, we tracked neuronal networks of three MEAs from 6 to 28 DIV. Spike detection efficiency was defined as the percentage of active electrodes out of 16 and 43 electrodes in microchannels and chambers, respectively. An electrode was counted as 'active' when mean firing rate was greater than 0.1 spikes/s. In Fig. 4(a), the percentages of active electrodes from three different networks are shown. Spontaneous activities were recordable as early as 9 DIV and the number of active electrodes increased over time in both areas. In microchannels, active electrodes were detected earlier and at least 30% of electrodes were active at 9–10 DIV, whereas only a few percent of electrodes were active in chambers. In addition, the number of active electrodes increased faster than those in chambers [see Fig. 4(b)]. The increment of active electrodes was larger in early periods, which reflected that many electrodes were detecting spikes in microchannels at early stages. The number of active electrodes reached its maximum value at 14–15 DIV in microchannels, whereas that in chamber was less than 40% in all MEAs at the same time point. After the dramatic increase of active electrodes in microchannels, they dropped between third and fourth weeks, whereas those in chamber increased gradually over four weeks without noticeable decrease. The earlier spiking activity from microchannels indicates that both chamber networks are active as early as 9 DIV, although there were few active electrodes in chambers. Between three to four weeks, the activity decreased only in microchannels even though axons appear to be intact until 28 DIV as shown in Fig. 2(b). This drop can occur when the signal propagation between chambers through the microchannels is reduced as the neuronal networks got matured due to the small number of interconnecting channels. A recent study reported that when the chambers were connected with a few microchannels, neuronal networks formed separated clusters as the neurons in each chamber were strongly connected among themselves [13].

E. Estimation of Axonal Conduction Velocity

To compute axonal conduction velocity, the cross correlogram between sorted units of two neighboring electrodes in the same microchannels was obtained. Next, we identified units from the same axon by screening a cross correlogram that had a unimodal shape with a maximum peak value larger than 10 counts per bin. The corresponding bin with the maximum peak was used as a delay time between the two units. Conduction velocity was estimated by dividing the distance between two neighboring electrodes, $200\,\mu\mathrm{m}$, by the delay time of each unit pair [see Fig. 5(a)]. Fig. 5(b) is a histogram of axonal delay at 14 DIV and 73% of identified pairs were in the range of 0.3–0.8 ms, which corresponded to the axonal velocities in the range of 0.2–0.5 m/s as shown in Fig. 5(c). The estimated velocity range was consistent with the values reported in other study using cortical neurons [7]. Fig. 5(d) shows axonal velocity plotted against the cultivation periods of 11, 14, 17, 21, and 24 DIV. According to the regression analysis, the axonal conduction velocity tended to increase with the cultivation days ($R^2 = 0.9912$). This implied that the axonal conduction became faster in cultured neuronal network as they got matured.

IV. Discussion

In this study, we established a two-compartment neural network connected with limited number of axons and characterized the neural spike recording from the network using planar-type MEA platform. It has been already shown that large axonal spikes could be recoded in microchannels (100–200 μV) [7]. What has not been investigated was whether there was a gain of SNR in microchannels. According to our electrical recordings from microelectrodes in microchannels, the high resistance ($\sim$1.9 MΩ) recording condition also increased background noise (11.0 $\mu\mathrm{V}_{(\mathrm{rms})}$), which was about two times larger than that in chambers. So, there was no significant improvement of SNR. However, considering the fact that it is very difficult to detect axonal spikes in open-chamber condition (SNR < 2) [4], locating microelectrodes in microchannels were highly effective in detecting axonal spikes (SNR ~ 13). In addition to the high signal quality, spike detection was more efficient in microchannels. The electrode coverage by cells was similar in microchannels and chambers [see Fig. 1(a)]. Axons were growing over the electrodes in microchannels, and somata or neurites were densely distributed on the MEA surfaces in chambers. Whereas axonal spikes were detected as early as at 9 DIV in microchannels, no spike was detected from microelectrodes in open-chamber area at the same time point [see Fig. 4(a)]. Earlier spike detection indicated that the spike activity in the network was present although it was not reported by electrodes in chambers. This implied that the axon guidance toward microelectrodes by microchannels would be an efficient way to interface neuronal networks for monitoring early neural activity.

Using this microchannel-based MEA platform, we calculated the velocity of signal propagation via axons in microchannels. About 73% of identified pairs were in the range of 0.2–0.5 m/s at 14 DIV and, in particular, the peak of velocity histogram was at 0.3–0.4 m/s. According to the literature, the mean velocity of the unmyelinated axons in hippocampal slices is 0.38 m/s [14]. It implies that the neural network formed in our platform had similar conduction properties to those in a slice culture preserving innate connectivity. From the axonal signals measured at 11, 14, 17, 21, and 24 DIV, the velocity tended to increase over the cultivation days. This is the first study that showed that the propagation through the axons becomes faster as the

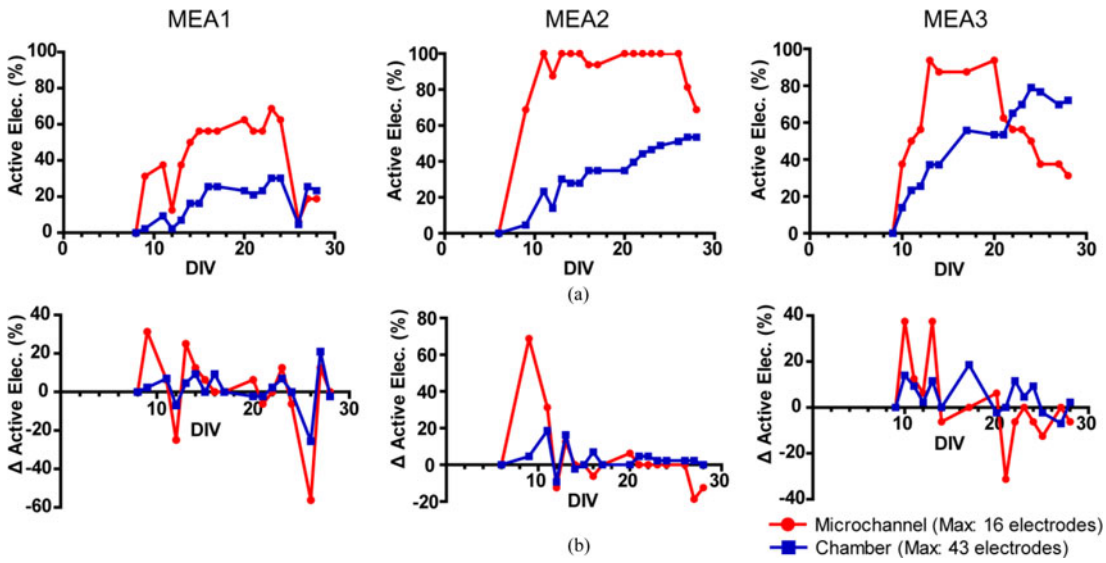

Fig. 4. Histogram (a) and increment (b) of active electrodes (>0.1 spikes/s) depending on cultivation days.

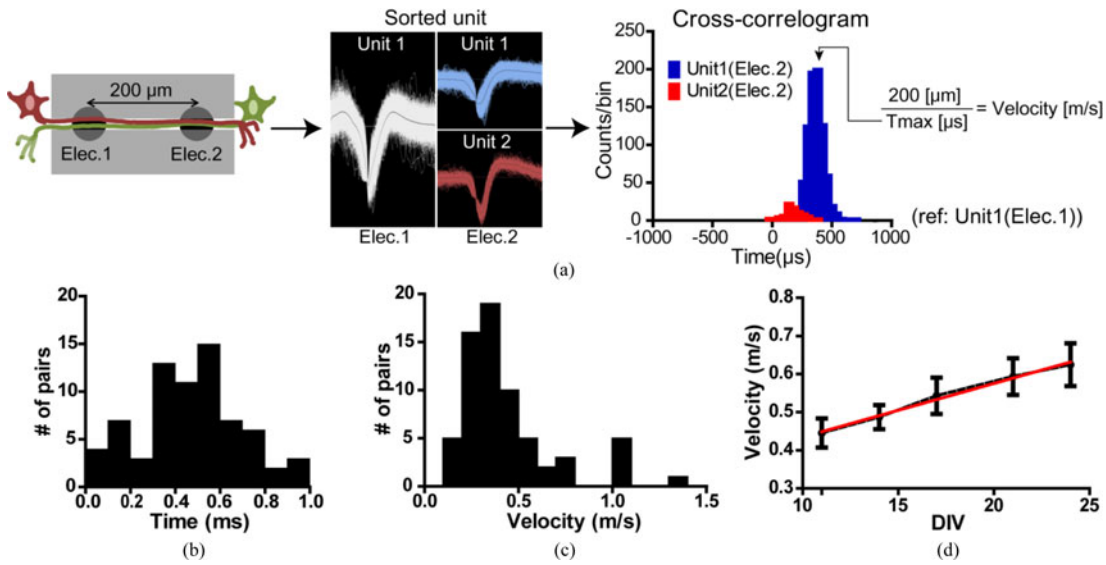

Fig. 5. (a) Schematics of estimating conduction velocity. Histogram of delay time (b) and conduction velocity (c) at 14 DIV. $N = 66$ pairs of identified units. (d) Linear regression of conduction velocity depending on cultivation days. $N = 42$, 66, 38, 30, 27 pairs of identified units. R^2: 0.9912.

network matures. Here, we can consider several factors that increased the conduction velocity of unmyelinated axons during the network development. First, it can be caused by the sodium currents that increased with the density of sodium channels [15]. This factor is thought to be one of the major parameters in this experimental condition, judging from the previous studies reporting that the amplitude and density of sodium current increased during the development in rat spinal and neocortical neurons [16]–[18]. Second, conduction velocity can be increased as the axon diameter increases which is directly correlated to resistance of the axoplasm. However, it is not considered as main factor because the increment of velocity in our result is much larger than the theoretical value, which is proportional to the square root of axonal diameters. Third possible factor can be an ephaptic interaction between axon fibers in microchannels. In our microchannels, unmyelinated axons were tightly packed and fasciculated into bundles, which was shown in Fig. 2(b). Such fasciculation could facilitate ephaptic interaction so that one active axon modulated excitability of adjacent axons [15]. It was reported in both experimental and computational studies that the subthreshold depolarization in ephaptic coupling in axons resulted in fast conduction velocity in excited axons nearby the coupled region [19]–[21]. Considering these results in previous studies, it may be responsible for the change of conduction velocity. Additionally, spiking behavior and potassium concentration can be considered as the factors affecting conduction velocity which were reported in recent studies [10], [22]. In contrast to our results, the decrease of conduction velocity was also reported. Jimbo *et al*. evaluated the conduction delay in distal part of axons and reported that the conduction velocity decreased over time in cultured neuronal network [9]. Compared to our study, they used different biological

preparations (hippocampus versus cortex, E18 rat versus E16 mouse), and their devices had wider and longer microchannels (width: $30\,\mu\mathrm{m}$, height: $5\,\mu\mathrm{m}$, length: $750\,\mu\mathrm{m}$) with much higher seeding density (5000 cells/mm^2). Swadlow showed that conduction velocity of most nonmyelinated axons was stable over the course of development in the intact brain [23]. In this previous research, their experimental conditions were different from our study (*in vitro* versus *in vivo*, hippocampal axons versus cerebral axons). However, further study is still needed to elucidate which factors increased the conduction velocity in network development and what was the reason for the different result from the previous study.

V. Conclusion

In this study, we designed and applied a microchannel device integrated on an MEA and axonal signals in microchannels and network-wide activity in chambers were successfully recorded. In microchannels, larger axonal signals were detected due to high resistance of microchannels with reasonable SNRs. Active electrodes were detected earlier in microchannels and the number of them increased faster than those in chambers. From the spikes detected in microchannels, the axonal conduction velocity was calculated to be 0.2–$0.5\ \mathrm{m/s}$ at 14 DIV, and showed a tendency to increase over cultivation days. The developed microchannel device integrated MEA is expected to be a useful platform for the studies of axonal spikes and their conduction.

References

[1] P. Erdi and T. Kiss, "The complexity of the brain: Structural, functional, and dynamic modules," in *Emergent Neural Computational Architectures Based on Neuroscience—Towards Neuroscience-Inspired Computing*, S. Wermter *et al.*, Ed. New York, NY, USA: Springer, 2001, pp. 203–211.

[2] D. Meunier *et al.*, "Modular and hierarchically modular organization of brain networks," *Front. Neurosci.*, vol. 4, pp. 200-1–200-11, Dec. 2010.

[3] D. Bucher and J. M. Goaillard, "Beyond faithful conduction: Short-term dynamics, neuromodulation, and long-term regulation of spike propagation in the axon," *Prog. Neurobiol.*, vol. 94. pp. 307–346, 2011.

[4] D. J. Bakkum *et al.*, "Tracking axonal action potential propagation on a high-density microelectrode array across hundreds of sites," *Nature Commun.*, vol. 4, no. 2181, pp. 2181-1–2181-12, 2013.

[5] A. M. Taylor *et al.*, "A microfluidic culture platform for CNS axonal injury, regeneration and transport," *Nature Methods*, vol. 2, pp. 599–605, 2005.

[6] J. W. Park *et al.*, "Microfluidic culture platform for neuroscience research," *Nature Protoc.*, vol. 1, pp. 2128–2136, 2006.

[7] B. J. Dworak and B. C. Wheeler, "Novel MEA platform with PDMS microtunnels enables the detection of action potential propagation from isolated axons in culture," *Lab Chip*, vol. 9, pp. 404–410, 2009.

[8] L. Pan *et al.*, "Large extracellular spikes recordable from axons in microtunnels," *IEEE Trans. Neural Syst. Rehabil. Eng.*, vol. 22, no. 3, pp. 453–459, May 2014.

[9] K. Shimba *et al.*, "Long term observation of propagating action potentials along the axon in a microtunnel device," in *Proc. 6th Int. IEEE/EMBS Conf. Neural Eng.*, San Diego, CA, USA, 2013, pp. 945–948.

[10] K. Shimba *et al.*, "Axonal conduction slowing induced by spontaneous bursting activity in cortical neurons cultured in a microtunnel device," *Integr. Biol.*, vol. 7, pp. 64–72, 2014.

[11] L. Pan *et al.*, "Propagation of action potential activity in a predefined microtunnel neural network," *J. Neural Eng.*, vol. 8, no. 4, pp. 046031-1–046031-12, 2011, Art. no. 046031.

[12] G. J. Brewer *et al.*, "Toward a self-wired active reconstruction of the hippocampal trisynaptic loop: DG-CA3," *Front. Neural Circuits*, vol. 7, no. 165, pp. 165-1–165-8, 2013.

[13] L. Pan *et al.*, "An *in vitro* method to manipulate the direction and functional strength between neural populations," *Front. Neural Circuits*, vol. 9, no. 32, pp. 32-1–32-14, 2015.

[14] J. P. Meeks and S. Mennerick, "Action potential initiation and propagation in CA3 pyramidal axons," *J. Neurophysiol.*, vol. 97, pp. 3460–3472, 2007.

[15] D. Debanne *et al.*, "Axon physiology," *Physiol. Rev.*, vol. 91, pp. 555–602, 2011.

[16] N. Alessandri-Haber *et al.*, "Specific distribution of sodium channels in axons of rat embryo spinal motoneurones," *J. Physiol.*, vol. 518, no. 1, pp. 203–214, Jul. 1999.

[17] B. V. Safronov *et al.*, "Axonal expression of sodium channels in rat spinal neurones during postnatal development," *J. Physiol.*, vol. 514, no. 3, pp. 729–734, Feb. 1999.

[18] J. R. Huguenard *et al.*, "Developmental changes in Na+ conductances in rat neocortical neurons: appearance of a slowly inactivating component," *J. Neurophysiol.*, vol. 59, pp. 778–795, 1988.

[19] J. D. Kocsis *et al.*, "Modulation of axonal excitability mediated by surround electric activity: An intra-axonal study," *Exp. Brain Res.*, vol. 47, pp. 151–153, 1982.

[20] M. Rasminsky, "Ephaptic transmission between single nerve fibres in the spinal nerve roots of dystrophic mice," *J. Physiol.*, vol. 305, pp. 151–169, 1980.

[21] R. C. Barr and R. Plonsey, "Electrophysiological interaction through the interstitial space between adjacent unmyelinated parallel fibers," *Biophys. J.*, vol. 61, pp. 1164–1175, 1992.

[22] M. K. Lewandowska *et al.*, "Cortical axons, isolated in channels, display activity-dependent signal modulation as a result of targeted stimulation," *Front. Neurosci.*, vol. 10, no. 83, pp. 83-1–83-14, 2016.

[23] H. A. Swadlow, "Physiological properties of individual cerebral axons studied *in vivo* for as long as one year," *J. Neurophysiol.*, vol. 54, pp. 1346–1362, 1985.

Nari Hong received the B.S. and M.S. degrees in bio and brain engineering from the Korea Advanced Institute of Science and Technology, Daejeon, South Korea, in 2013 and 2015, respectively, where she is currently working toward the Ph.D. degree in bio and brain engineering.

Her research interests include design of *in vitro* neural network model.

Sunghoon Joo received the B.S. and M.S. degrees in bio and brain engineering from the Korea Advanced Institute of Science and Technology, Daejeon, South Korea, in 2011 and 2013, respectively where he is currently working toward the Ph.D. degree in bio and brain engineering.

His research interests include neural network design and analysis, microfabrication for *in vitro* neurobiology.

Yoonkey Nam (S'01–M'06) was born in South Korea in 1973. He received the B.S degree from the Seoul National University, Seoul, South Korea, in 1997 and the M.S and Ph.D. degrees in electrical engineering from the University of Illinois at Urbana-Champaign, Urbana, IL, USA, in 2003 and 2005, respectively.

Since 2006, he has been with Korea Advanced Institute of Science and Technology, where he is currently an Associate Professor of bio and brain engineering, and a Member of brain and cognitive engineering program. His research interests include surface biofunctionalization, micropatterning technology for neuronal networks, microelectrode arrays, multichannel neural signal analysis, neurophotonics, and nano-scale neural interfaces, which are aimed at engineering *in vitro* neural interfaces for Brain-on-a-Chip technology.